



**Claire Froger<sup>1</sup>, Nicolas P. A. Saby<sup>1</sup>, Claudy C. Jolivet<sup>1</sup>, Line Boulonne<sup>1</sup>, Giovanni Caria<sup>2</sup>, Xavier Freulon<sup>3</sup>, Chantal de Fouquet<sup>3</sup>, H  l  ne Roussel<sup>4</sup>, Franck Marot<sup>4</sup>, and Antonio Bispo<sup>1,4</sup>**

<sup>4</sup>ADEME International, 20 Ave Gresille, 49004 Angers 01, 75006 Paris, France

Revised: 12 April 2021 – Accepted: 22 April 2021 – Published: 2 June 2021

Published by Copernicus Publications on behalf of the European Geosciences Union.

The various studies that can be found in the literature on PAH soil contamination mainly focus on local soil pollution (Liu et al., 2016; Yang et al., 2008) or on soils under a particular type of land use (Cachada et al., 2012a; Jensen et al., 2007; Wang et al., 2017a). To efficiently manage soil contamination and prevent the release of pollutants stored in soils, we need to work at the scale of countries to determine the spatial variations in these contaminants and evaluate their risks to both ecosystems and human populations.

To fully understand the spatial distribution of PAHs, especially at a national scale, we need to determine the origin of the contaminants to potentially enact mitigation techniques at their sources. Considering the widespread contamination of western Europe by the PAHs released since 1850 (Fernández et al., 2000), it is necessary to determine whether the contamination of soils observed nowadays is the result of legacy pollution or the current release of these substances. Multiple tracing methods have been developed to identify PAH sources. Among these techniques, PAH molecular ratios have been widely used to discriminate PAHs according to their pyrogenic and petrogenic origins (Ravindra et al., 2008; Yunker et al., 2002); however, these PAH ratios appear to be sensitive to environmental processes such as oxidation and photo-oxidation, resulting in their modification during PAH transport due to the preferential degradation of some PAHs (Biache et al., 2014; Zhang et al., 2005). To prevent misinterpretations, the use of a combination of multiple PAH ratios is necessary to more accurately identify the origin of PAHs (Kavouras et al., 2001; Tobiszewski and Namieśnik, 2012).

Due to health issues that are attributed to PAHs, an assessment of risks posed by contaminated soil to humans needs to be conducted to proceed with land management decisions. The United States Environmental Protection Agency (USEPA) developed guidelines to conduct human health risk assessments prior to the remediation of contaminated sites (USEPA, 1991), and they then created a manual for soil screening (USEPA, 1996). Improvements were made to adapt the risk assessment to the various types of soil contaminant exposure, including residential, occupational, and recreational exposure (USEPA, 1996, 2020). In addition, the parameters used in the risk calculations are regularly updated based on the results reported in the literature (IRIS, NCEA, and U.S. EPA, 2008). Therefore, a health risk assessment has been applied in multiple studies addressing PAHs in soils (Albanese et al., 2015; Cachada et al., 2016; Wang et al., 2017b), using a determinist point estimate approach to first evaluate the health risks posed by soils, as recommended by the USEPA (2001).

Only a handful of studies have examined PAHs in soils at national scales, such as those in the United Kingdom (Heywood et al., 2006), China (Ma et al., 2015), Switzerland (Desaules et al., 2010), Germany (Aichner et al., 2013), and the Netherlands (Brus et al., 2009). Unfortunately, the selected sampling design (e.g. Brus et al., 2009), soil sampling

resolution, or land use specifications (Aichner et al., 2013) have limited the use of these relevant data sets for accurately mapping the PAH spatial distribution at national scales. Currently, only Villanneau et al. (2013) have attempted to map the distribution of a selection of PAHs in French soils based on a coarse sampling grid corresponding to a subset of 549 soils collected within the framework of the French Soil Quality Monitoring Network (RMQS – Réseau de Mesure de la Qualité des Sols). Their paper provided a first look at the spatial distribution of PAHs at the national scale; however, only four compounds (benzo(b)fluoranthene, fluoranthene, pyrene, and phenanthrene) met the criteria to be mapped using geostatistical technics. The four resulting maps showed a general trend of PAHs in French soils but only broad-scale spatial variation were detected in PAHs contamination due to the low resolution of the input data. As this first work gave limited insights to the identification of PAH origins and their distribution, working with the sum of all PAH molecules is therefore necessary to look further into PAH distribution over the territory and to identify their origins.

Finally, of the large-scale studies of PAHs in soils that have been reported, the spatial distribution and contaminant levels have been the main focus, while health risk assessments and source identification have only been assessed at local scales (Morillo et al., 2008; Wang et al., 2015, 2013). Therefore, it is necessary to conduct complete studies at national scales, including the identification of major PAH sources to understand their spatial distribution and an evaluation of the associated risks to build effective national policies.

The objectives of the current study are, thus, (i) to evaluate the contamination of soils by PAHs in France in comparison with international soil monitoring studies, (ii) to produce a high-resolution map of the spatial distribution of  $\Sigma 15$ PAHs in French soils, (iii) to determine the main origins of PAHs in soils based on PAH molecular ratios, and (iv) to evaluate the potential health risks for the residential population associated with PAHs in French soils in order to have a first look at the risks induced by the background contamination of soils.

## 2 Materials and methods

### 2.1 Sampling sites

The sampling sites were selected based on a regular grid of 16 km  $\times$  16 km, and they were sampled at the centre of each cell or in a radius of less than 1 km from the theoretical centre when no soil was found at the predicted location (Fig. S1). Approximately 2200 sites were sampled, which consisted mostly of agricultural lands (50 %), grasslands (20 %), and forests (25 %), with 1.2 % of the region being urbanised areas (including brownfields) and 2.7 % of the region being natural areas.

## 2.2 Sampling procedure and analysis

The sampling procedure and PAH analyses have been detailed in Villanneau et al. (2009, 2013); the soils were sampled from June 2000 to May 2010, using a systematic procedure. At each site, in a  $20\text{ m} \times 20\text{ m}$  grid, 25 core samples of topsoil (approximately 0–30 cm) were taken. The core samples were bulked to obtain a composite sample, which was air-dried and sieved to 2 mm before analysis.

The concentrations of the following 16 PAH compounds were measured in the topsoil composite samples: naphthalene (Naph), acenaphthylene (Acy), acenaphthene (Ace), fluorene (Flu), phenanthrene (Phe), anthracene (Ant), fluoranthene (Flh), pyrene (Pyr), benzo(a)anthracene (BaA), chrysene (Chry), benzo(b)fluoranthene (BbF), benzo(k)fluoranthene (BkF), benzo(a)pyrene (BaP), dibenzo(ah)anthracene (DahA), indeno(123,cd)pyrene (IndP), and benzo(ghi)perylene (BghiP). These analyses were conducted at the Laboratory of Soils Analysis of the National Research Institute of Agronomy (INRA, in French) in Arras, France; this laboratory is accredited for PAH analysis in soils by the French accreditation committee (COFRAC). All the analyses were conducted between 2008 and 2012; consequently, volatilisation of lighter PAHs, such as Naph, could have occurred during the long-term storage of soils collected at the beginning of the sampling campaign.

A subsample of  $\sim 20\text{ g}$  was taken from topsoil composites, and PAHs were extracted using a Dionex ASE 200 extractor to perform pressure liquid extraction at high pressure (103.4 bar) and temperature ( $150^\circ\text{C}$ ), with a mixture of acetone / hexane / dichloromethane (50/25/25;  $v/v/v$ ). After extraction, the samples were partially concentrated by rotary evaporation to a volume of 5 mL and then completely evaporated under a gentle flow of nitrogen. The dry residue was taken up with 2 mL of methanol and filtered through a  $0.2\text{ }\mu\text{m}$  PTFE (polytetrafluorethylene) filter to remove solid particles, which were finally transferred into 2 mL vials. The extracts were then injected into a thermoelectric high-performance liquid chromatograph (HPLC) with a quaternary pump P4000, an autosampler AS3000, a commutator SN4000 coupled with two thermoelectron detectors mounted in series, a diode array ultraviolet (UV6000), and a spectrofluorimeter (F3000). A  $10\text{ }\mu\text{L}$  volume aliquot was injected in the HPLC, and the PAHs were separated on a Hypersil PAH column (100 mm in length;  $0.46\text{ mm}$  diameter;  $5\text{ }\mu\text{m}$  particle size) of a  $\text{C}_{18}$  reversed phase. In-depth technical details of the chromatographic parameters used are provided by Villanneau et al. (2009).

External calibration was used to quantify PAHs with concentrations from 40 to  $1000\text{ }\mu\text{g L}^{-1}$  detected by fluorescence, except for acenaphthylene and indeno(123,cd)pyrene, which were detected by ultraviolet irradiation. The limits of quantification (LOQ) were  $0.005\text{ mg kg}^{-1}$  for fluorene and anthracene;  $0.01\text{ mg kg}^{-1}$  for acenaphthene, phenanthrene, fluoranthene, pyrene,

benzo(a)anthracene, benzo(b)fluoranthene, benzo(a)pyrene, and indeno(123,cd)pyrene;  $0.02\text{ mg kg}^{-1}$  for naphthalene and dibenzo(ah)anthracene;  $0.03\text{ mg kg}^{-1}$  for acenaphthylene; and  $0.05\text{ mg kg}^{-1}$  for chrysene, benzo(k)fluoranthene, and benzo(ghi)perylene. The complete method for PAH analysis is referenced in the European analytical standard (NF EN 16181; AFNOR, June 2018). The analyses were validated using a reference material (values reported in Table S1) which has been systematically added to the sequence of soil sample analyses to validate the results. Of the 16 PAHs measured, one acenaphthylene could not be validated by the reference material (i.e. value of  $0\text{ mg kg}^{-1}$  for the reference material; see Table S1). Therefore, compound Acy quantified only in 1 % of the soil samples was excluded from the study when considering the remaining 15 PAHs.

Finally, the expanded uncertainty was estimated for every PAH through repeatability and reproducibility tests, using a coverage factor of two, which gives a confidence level of 95 % (Table S2). In addition, the loss of the most volatile compound Naph could have occurred due to the soil sampling technique using composite samples and due to the soil analysis occurring years after the original sample collection. In addition, to avoid overestimation of the total PAH content, values under the LOQ were considered to have no PAH content (i.e.  $0\text{ }\mu\text{g kg}^{-1}$ ).

## 2.3 Geostatistical modelling

A geostatistical modelling approach was used to map the  $\Sigma 15$  PAHs and their probability of exceeding a selected threshold (Webster and Oliver, 2007). The observations include many null values (30 %) that correspond to values under the LOQ. They also demonstrate extreme values due to locally distinct processes, such as point pollution from industrial sites. For zero-inflated and heavy-tailed distributions, standard geostatistical methods are not the most appropriate because they often lead to poor estimates. In addition, these methods do not properly handle the mapping of risks. Non-linear methods such as indicator kriging, disjunctive kriging, or conditional expectation have been developed for such cases and have found wide acceptance in soil science (Chilès and Delfiner, 2012; Emery, 2006; Rivoirard, 1994). In this study, the total PAHs were modelled as a transform of a normal Gaussian field,  $Z = \phi(Y)$ . The spatial structure of the Gaussian field is first determined, and then maps of either the total PAHs or the risk of exceeding a threshold are computed by conditional expectation.

In the case of continuous distribution of the original data, the anamorphosis function strictly increases and can be inverted to assign to each observed value its Gaussian counterpart. Then, a common method for variogram estimation can be used (e.g. to calculate the empirical and/or experimental variogram by the method of moments and then to fit a model to the empirical variogram via nonlinear least squares). Here, the proportion of null values is  $p_0 = 30$ ; hence, the transfor-

mation function  $\phi$  is identically equal to 0 for all Gaussian values lower than the Gaussian quantile  $y_0 = G^{-1}(p_0)$ . It follows that the actual value of  $Y$  is unknown, where  $Z = 0$ , but is only constrained by the inequality  $Y < y_0$ .

In such a case, two preliminary steps must be performed, namely determining the covariance of  $Y$  and then assigning a Gaussian value to each data point at which  $Z$  is null. For the first step, the zero-inflated distribution of the original data is transformed into an inflated Gaussian distribution with an inflated value equal to the quantile of the proportion of observed null values,  $y_0$  (a normal score is applied, and then, all values below  $y_0$  are set to this value). Then, to estimate the covariance function of the Gaussian field, the empirical variogram of the inflated Gaussian variable is computed, and the model of the Gaussian field (without inflated values) is fitted by nonlinear least squares, taking into account the relationship between the covariances between the Gaussian variables and the covariances between the transformed variables. Once the structure of  $Y$  is determined, the second step consists of simulating the values of the Gaussian field where the  $\Sigma 15$  PAH value is null, honouring the spatial structure and the inequality constraint. This is classically performed using a Gibbs sampler (Petitgas et al., 2017).

The validity of the best-fitted geostatistical model was then assessed in terms of the standardised squared prediction error (SSPE) using the results of a  $k$ -fold cross-validation. If the fitted model was a valid representation of the spatial variation in the Gaussian variable, then the sum of the squares of the errors would have an approximate  $\chi^2$  distribution with a mean of 1 and a median of 0.455 (Lark, 2002).

As both the variogram model and the value of the Gaussian field at all data points are defined, the conditional expectation, also called the multi-Gaussian kriging, can be calculated to map the total PAHs. The simple kriging of the Gaussian variable is computed first, and then, the conditional expectation of any transform of the Gaussian field is derived using the following:

$$\psi(Y_s)\}^{\text{CE}} = \int_{-\infty}^{+\infty} \psi(y_s^{\text{SK}} + \sigma_{SK}u) g(u) du, \quad (1)$$

where  $y_s^{\text{SK}}$  and  $\sigma_{SK}$  are, respectively, the kriging value at location  $s$  (the nodes of the grid) and the standard deviation of the kriging error. The transform function  $\psi$  can be either the initial anamorphosis to map the total PAHs or the indicator  $y \rightarrow 1_{y \geq \phi^{-1}(z_c)}$  to map the risk that the variable exceeds the threshold  $z_c$ . However, these estimates rely on the Gaussian values being simulated when the original values are null, and these simulated values are used for the kriging computation. Thus, the final estimate is established by the total expectation formula, where the expectation over the Gaussian values constrained by the inequalities is computed by a Monte Carlo integration, i.e. averaging different outcomes produced by the Gibbs sampler.

The geostatistical analysis and the linear and nonlinear predictors were performed using the R software RGeostats package (MINES ParisTech/ARMINES, 2020).

## 2.4 Health risk assessment

From a toxicological standpoint, PAHs exhibit threshold and nonthreshold effects. The risks for residential populations were estimated based on lifetime exposure; for such a duration of exposure, the risks are mainly induced by nonthreshold effects. For the ranges of the concentrations measured in soils, it has been verified that the threshold effects are never exceeded, even for shorter exposures, including for children. Thus, only the nonthreshold effects of PAHs were considered in the context of this study. The estimation of cancer risk associated with the exposure of individuals to potentially carcinogenic pollutants in French soils was calculated based on the equations developed by the USEPA (USEPA, 1991) and used in several studies (Cachada et al., 2016; Wang et al., 2017a; Yang et al., 2014). The incremental lifetime cancer risks (ILCRs) were calculated for each of the three pathways, i.e. soil ingestion, dermal absorption, and soil particle inhalation. To perform the risk assessment, we converted the concentrations of PAHs measured in every soil sample into a BaP equivalent concentration (i.e.  $\text{BaP}_{\text{eq,soil}}$ ) using the following:

$$\text{BaP}_{\text{eq,soil}} = \sum_{i=1}^n \text{PAH}_i \times \text{TEF}_i, \quad (2)$$

with  $\text{BaP}_{\text{eq,soil}}$  being the BaP equivalent concentration in soil in milligrams per kilogram,  $\text{PAH}_i$  is the concentration of the  $i$ th PAH molecule in the soil (milligrams per kilogram), and  $\text{TEF}_i$  is the toxic equivalent factor for the  $i$ th PAH molecule (see Table S3 in the Supplement).

We estimated the lifetime cancer risk for the residential population (children and adults) living in the area of the sampling site by considering only their direct exposure to contaminated soil (without the ingestion of vegetables collected from the garden). We assumed the local homogeneity of PAHs in soils, considering the PAH concentrations in French soils measured in the current study as the background exposure, and, therefore, focused on the long-term impacts on the population (i.e. nonthreshold effects).

Table 1 presents the equations used to calculate the ILCRs for the residential population, and Table 2 details the values of parameters used in the calculations based on the risk assessment guidance of USEPA (1991, 1996, 2020).

The total lifetime cancer risk (TLCR) was calculated by summing the three ILCRs for the residential population and outdoor workers.



**Table 1.** Equations used for the health risk assessment of the residential population.

Pathway	Residential population
Ingestion	$\text{ILCR}_{\text{ing, res}} = \frac{C_{\text{soil}} \times \text{IF}_{\text{soil/adj}}}{\text{AT} \times 10^6} \times \text{CSF}_0,$ <p>where</p> $\text{IF}_{\text{soil/adj}} = \left( \frac{\text{EF}_{\text{c, res}} \times \text{ED}_{\text{c, res}} \times \text{IRS}_{\text{c, res}}}{\text{BW}_{\text{c}}} + \frac{\text{EF}_{\text{a, res}} \times (\text{ED}_{\text{a, res}} - \text{ED}_{\text{c, res}}) \times \text{IRS}_{\text{a, res}}}{\text{BW}_{\text{a}}} \right).$
Dermal	$\text{ILCR}_{\text{der, res}} = \frac{C_{\text{soil}} \times \text{DFS}_{\text{soil/adj}} \times \text{ABS}_{\text{d}}}{\text{AT} \times 10^6} \times \frac{\text{CSF}_0}{\text{GIABS}},$ <p>where</p> $\text{DFS}_{\text{soil/adj}} = \left( \frac{\text{EF}_{\text{c, res}} \times \text{ED}_{\text{c, res}} \times \text{SA}_{\text{c, res}} \times \text{AF}_{\text{c, res}}}{\text{BW}_{\text{c}}} + \frac{\text{EF}_{\text{a, res}} \times (\text{ED}_{\text{a, res}} - \text{ED}_{\text{c, res}}) \times \text{SA}_{\text{a, res}} \times \text{AF}_{\text{a, res}}}{\text{BW}_{\text{a}}} \right).$
Inhalation	$\text{ILCR}_{\text{inh, res}} = \frac{C_{\text{soil}} \times \text{EF}_{\text{a, res}} \times \text{ED}_{\text{a, res}} \times \text{ET}_{\text{a, res}} \times (1/\text{PEF})}{\text{AT}} \times \text{IUR}.$
Total	$\text{TLCR}_{\text{res}} = \text{ILCR}_{\text{ing, res}} + \text{ILCR}_{\text{der, res}} + \text{ILCR}_{\text{inh, res}}.$

**Table 2.** Detailed parameters used in the incremental lifetime cancer risk assessment based on USEPA (2020).

Parameter		Units	Value
AT	Averaging time	d	25 550 (365 × 70)
EF <sub>c, res</sub>	Exposure frequency (child)	d yr <sup>-1</sup>	350
ED <sub>c, res</sub>	Exposure duration (child)	yr	6
IRS <sub>c, res</sub>	Soil ingestion rate (child)	mg d <sup>-1</sup>	200
BW <sub>c</sub>	Body weight (child)	kg	15
EF <sub>a, res</sub>	Exposure frequency (adult)	d yr <sup>-1</sup>	350
ED <sub>a, res</sub>	Exposure duration (adult)	yr	70
IRS <sub>a, res</sub>	Soil ingestion rate (adult)	mg d <sup>-1</sup>	100
BW <sub>a</sub>	Body weight (adult)	kg	60
SA <sub>c, res</sub>	Surface area (child)	cm <sup>-2</sup>	2373
AF <sub>c, res</sub>	Adherence factor (child)	mg cm <sup>-2</sup>	0.2
SA <sub>a, res</sub>	Surface area (adult)	cm <sup>-2</sup>	6032
AF <sub>a, res</sub>	Adherence factor (adult)	mg cm <sup>-2</sup>	0.07
ABS <sub>d</sub>	Dermal absorption factor		0.13
GIABS	Gastrointestinal absorption factor		1
PEF	Particle emission factor	m <sup>3</sup> kg <sup>-1</sup>	1.32 × 10 <sup>9</sup>
CSF <sub>0</sub>	Cancer oral slope factor	(mg kg <sup>-1</sup> d <sup>-1</sup> ) <sup>-1</sup>	1
IUR	Inhalation unit risk	(mg m <sup>-3</sup> ) <sup>-1</sup>	0.6

### 3 Results and discussion

#### 3.1 PAH contents and the influence of soil characteristics

##### 3.1.1 PAH concentrations and composition

Descriptive statistics of the data set are presented in Table 3, showing summary statistics for each PAH molecule and for the sum of the 15 PAHs. Over the 2154 soils sampled, PAHs (at least one molecule) could be quantified in 1512 soils corresponding to 70 % of the samples. Among the 1512 soils with measurable PAH concentrations, 732 contained more than six PAH molecules above the LOQ.

Fluoranthene and phenanthrene were quantified in 56 % and 55 % of the soil samples (Table 4), respectively, followed by benzo(b)fluoranthene (48 %) and pyrene (46 %).

Conversely, acenaphthene was measured in less than 2 % of the total soil samples.

The results highlight the large differences between the levels of soil contamination, with PAH concentrations varying from 5.1 to 31 200 µg kg<sup>-1</sup> in the Σ15 PAHs. However, extreme values were not frequent, as 90 % of the PAH concentrations measured were under 500 µg kg<sup>-1</sup> in the Σ15 PAHs, and only 4 % of the concentrations were above 1000 µg kg<sup>-1</sup> in the Σ15 PAHs.

The concentrations of the Σ15 PAHs measured in the current study were in the same range as the PAH contents measured in rural soils from various locations in Europe and China (Table 4), which also demonstrated large variations in the Σ15 PAH concentrations. The highest concentrations reported in the literature were mostly attributed to local sources, such as urban and industrial areas. Results similar

**Table 3.** Summary of descriptive statistics in micrograms per kilogram.

PAH molecule	<i>N</i> > LOQ	<i>N</i> > LOQ (%)	SD or mean	Min	<i>Q</i> <sub>25</sub>	<i>Q</i> <sub>50</sub>	<i>Q</i> <sub>75</sub>	Max	Mean
Naphthalene	127	6	9.5	< LOQ	< LOQ	< LOQ	< LOQ	1030	2.7
Acenaphthene	38	2	13.1	< LOQ	< LOQ	< LOQ	< LOQ	160	0.3
Fluorene	231	11	6.1	< LOQ	< LOQ	< LOQ	< LOQ	250	1.4
Phenanthrene	1176	55	4.7	< LOQ	< LOQ	11.2	19.275	3470	19.0
Anthracene	174	8	10.4	< LOQ	< LOQ	< LOQ	< LOQ	555	1.9
Fluoranthene	1201	56	5.1	< LOQ	< LOQ	12.05	26	6080	30.3
Pyrene	996	46	5.1	< LOQ	< LOQ	< LOQ	19.575	4370	22.4
Benzo(a)anthracene	559	26	5.5	< LOQ	< LOQ	< LOQ	10.2	2180	11.3
Chrysene	180	8	9.0	< LOQ	< LOQ	< LOQ	< LOQ	4140	11.3
Benzo(b)fluoranthene	1039	48	3.6	< LOQ	< LOQ	< LOQ	18.5	2220	18.0
Benzo(k)fluoranthene	825	38	< 4.9	< LOQ	< LOQ	< LOQ	8.0675	1460	8.2
Benzo(a)pyrene	658	31	4.7	< LOQ	< LOQ	< LOQ	12.3	1730	12.8
Dibenzo(ah)anthracene	148	7	8.6	< LOQ	< LOQ	< LOQ	< LOQ	1130	3.5
Indeno(123cd)pyrene	655	30	4.7	< LOQ	< LOQ	< LOQ	12.1	1830	10.8
Benzo(ghi)perylene	135	6	6.8	< LOQ	< LOQ	< LOQ	< LOQ	1530	7.2
Σ15 PAHs	1512	70	5.1	< LOQ*	< LOQ*	32.6	121.8	31 193	161.0
BaPeq	1512	70	5.2	< LOQ*	< LOQ*	1.13	17.5	3705	21.4
Two–three-ring PAHs (%)				NA	NA	10.3	21.3	100	18.5
Four-ring PAHs (%)				NA	NA	36.3	49.2	100	28.9
Five–six-ring PAHs (%)				NA	NA	22.8	39.8	100	22.7

\* For the sum of the 15 PAHs, < LOQ means that no PAH molecules were quantified. NA – not available.

to those in this study were found in Poland with respect to the PAH distribution, with 75 % of the soil samples being characterised by PAH content  $\leq 694 \mu\text{g kg}^{-1}$  (Maliszewska-Kordybach et al., 2008).

### 3.1.2 Influence of soil physicochemical parameters

The PAHs measured in the samples were mostly four- and five–six-ring PAHs, respectively, representing median values of 36 % and 23 % of the total PAHs, with the two–three-ring PAH contribution being around 10 % (Table 4). These observations are in accordance with the literature values showing a lower content of light PAHs in soils over time and a stable content of heavy PAHs (Cui et al., 2020; Gubler et al., 2015). The sorption of PAHs on organic matter due to their lipophilic properties is known to be a key factor in PAH evolution in soils (Maliszewska-Kordybach et al., 2008; Yu et al., 2018). As the soil organic matter structure is strongly influenced by pH, the fate of PAHs could also be influenced by the soil pH, especially in forest soils (Aichner et al., 2013; Wenzel et al., 2002). Nevertheless, in the current study, no clear influence of organic carbon, organic matter (when available), or pH on the PAH content was evident, except for in urban parks (see Figs. S2, S3, and S4 in the Supplement). The low or nonexistent impact of soil characteristics on the PAH concentrations found in multiple studies (Aichner et al., 2013; Maliszewska-Kordybach et al., 2008) could be attributed to the stronger influence of other factors, such as source proximity and meteorological parameters (Heywood et al., 2006; Lohmann et al., 2000). In soils receiving iden-

tical amounts of PAHs emitted by anthropogenic activities, local variations in the pH and total organic carbon might exert an influence on the fate of those contaminants in soils (Wenzel et al., 2002). This is supported by the correlation between the PAH content and soil characteristics for soils in urban parks, as urban areas have highly concentrated PAH emissions from sources such as road traffic, industries, and residential emissions (Cachada et al., 2012b; Keyte et al., 2016). However, considering that five soils in this study were collected from urban parks, a similar conclusion cannot be made based on our data set. At the scale of the entire country, the influence of soil characteristics on PAH content would be minimised by the proximity of major emission sources (Aichner et al., 2013).

In addition to soil physicochemical characteristics, relationships between the PAH content in soils and land use type have been noted in some studies (Maliszewska-Kordybach, 1999); however, no differences in PAH content were observed among forests, cultivated lands, and permanent pastures in this study (see Fig. S4 in the Supplement). Only soil located in natural areas seems to present a lower content of PAHs (Kruskal–Wallis test; *p* value < 0.05), but these results should be considered with caution since the number of natural areas accounted for less than 5 % of the 2154 sites (Sect. 2.1). Therefore, agricultural practices appear to have a minor influence on the PAH concentrations measured in French soils.

**Table 4.** PAH concentrations in soils reported in the literature in micrograms per kilogram.

	Location	Land use type	Concentrations in $\mu\text{g kg}^{-1}$	No. of PAHs considered	
France	This study		5.1–31 193	15	
	Orgeval	Rural ( $n = 25$ ) Urban ( $n = 8$ )	60–5305	13	Gateuille et al. (2014b)
	Rouen	Rural (forest)	450–5650	14	Motelay-Massei et al. (2004)
	Paris conurbation	Rural ( $n = 12$ ) Urban ( $n = 20$ )	150–55 000	15	Gaspéri et al. (2018)
Norway	Transect to Oslo	Forest soils	10–2600	16	Jensen et al. (2007)
Poland	Entire country	Rural ( $n = 217$ )	80–7264	16	Maliszewska-Kordybach et al. (2008)
Switzerland	Entire country	Urban ( $n = 2$ ) Semi-rural ( $n = 13$ ) Rural ( $n = 7$ ) Remote ( $n = 1$ )	19–6870	16	Gubler et al. (2015)
Germany	Entire country	Forest soils ( $n = 447$ )	105–14 889	16	Aichner et al. (2013)
UK	England, Scotland, Wales, and Northern Ireland	Rural ( $n = 122$ )	24–128 000 (mean – 608)	16	Bull and Collins (2013)
China	Entire country	Rural ( $n = 120$ ) Urban ( $n = 28$ )	9.9–5910 (mean – 377)	16	Ma et al. (2015)
	Dongjiang River basin	Rural ( $n = 30$ )	23.5–231 (mean – 116)	16	Zheng et al. (2014)

### 3.2 Spatial distribution of PAHs

#### 3.2.1 PAH-level distribution over France

In this study, we provide the first national map of the  $\Sigma 15$  PAHs in Fig. 2a using multi-Gaussian kriging, which is a standard and versatile method. Once the kriging of the Gaussian variable is computed, maps for various transform functions can be easily derived. Here, it is particularly difficult to properly handle the LOQ, so a Monte Carlo integration was added for this purpose.

No evident anisotropy can be seen on the sample variogram; the omnidirectional estimated variogram and fitted model are shown in Fig. 2c. The variogram displays a very large nugget effect, showing the substantial short-range variability for the  $\Sigma 15$  PAHs induced by the contamination process. A nested model was used to combine a nugget and a spherical model (range of 488 km). The conditional expectation approach assumes a stationary Gaussian field model. To meet this assumption, we forced the sill of the variogram model to 1, which corresponds to the total variance of the normally scored transformed variable. Notably, the estimated variogram continuously increases after 400 km, which corresponds to the north-to-south gradient observed in the data; however, this issue could be easily solved via point kriging,

with a moving 250 km radius neighbourhood and a maximum of 150 data points (Rivoirard and Romary, 2011) so that only the well-fitted part of the variogram intervenes. The results of the 10-fold cross-validation gave a mean SSPE value of 0.92 and a median SSPE value of 0.447, with both values falling within the confidence interval of the theoretical values. Finally, the  $R^2$  in the transformed space equalled 0.33.

The spatial distribution of the PAH concentrations in French soils highlighted wide variations in the contamination throughout the French territory. The northeastern part of France, known to be an industrialised region, showed the highest levels of PAHs in the soils, as noted by Villanneau et al. (2013) for benzo(b)fluoranthene, fluoranthene, pyrene, and phenanthrene. In addition, higher PAH concentrations could be observed in the region of the Rhône valley, which is also known to be industrialised, and around major harbour cities along the west coast (Fig. 1b). Finally, hot spots of PAHs were found near major cities such as Paris, Marseille, Lyon, Nantes, and Bordeaux (Fig. 1a). Those late observations contradict the results of Villanneau et al. (2013), showing mostly the northeastern–southwestern gradient without any evidence of the cities' impacts on soil contamination by PAHs.

To evaluate the state of contamination of the French soils, PAH concentrations should be compared with international

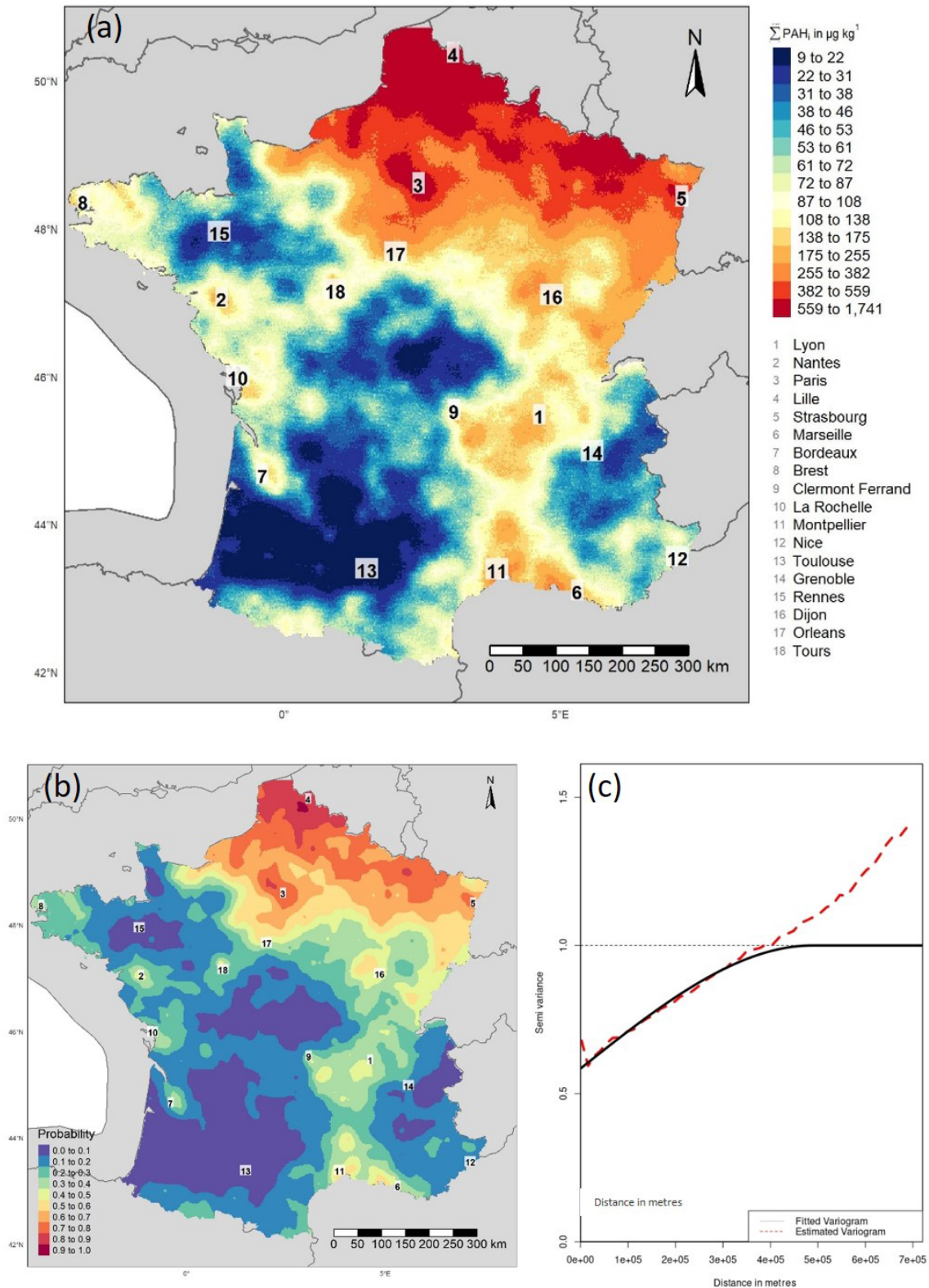


**Figure 1.** (a) The estimated spatial distribution of the total PAH ( $\Sigma 15$  PAHs) concentrations in micrograms per kilogram by conditional expectation, along with major cities in France. (b) Map of the estimated probability of exceeding  $100 \mu\text{g kg}^{-1}$  in the  $\Sigma 15$  PAHs. (c) Estimated (in red) and fitted (in black) variograms of the normally scored transformed  $\Sigma 15$  PAHs.



**Table 5.** The soil contamination classification suggested by Maliszewska-Kordybach (1996) and a design-based estimation of the proportion of associated French soils.

Soil classification	PAH ranges ( $\mu\text{g kg}^{-1}$ )	Proportion of French soils (in %)
Noncontaminated	< 200	83
Weakly contaminated	200–600	12
Contaminated	600–1000	2.1
Heavily contaminated	> 1000	2.9

historical background values, as PAHs could be emitted by natural sources such as wild fires during the Jurassic period (Killops and Massoud, 1992). Some studies have suggested a lower limit of  $100 \mu\text{g kg}^{-1}$  in the total PAHs, as in Canada (Canadian Council of Ministers of the Environment, 2010) or in the Seine river basin (Gaspéri et al., 2018; Gateuille et al., 2014b). Maliszewska-Kordybach (1996) suggested a classification of agricultural soils in Poland based on the  $\Sigma 15$  PAHs concentrations, as presented in Table 5.

The values outlined in Table 5 are supported by studies of preindustrial periods (i.e. before 1830), such as Fernández et al. (2000), which showed PAH concentrations of  $20\text{--}100 \mu\text{g kg}^{-1}$  in 1830 in lake sediment cores across Europe. Other studies reported PAH concentrations under  $200 \mu\text{g kg}^{-1}$  in sediments from 1400 to 1850 (Elmqvist et al., 2007; Leorri et al., 2014).

Based on the classification of Maliszewska-Kordybach (1996), the proportions of French soils attributed to each soil class were calculated (Table 5), showing that 17 % could be considered contaminated when using a threshold value of  $200 \mu\text{g kg}^{-1}$ . When applying the Canadian background value of  $100 \mu\text{g kg}^{-1}$  (Table 5), 30 % of the French soils could be considered contaminated (i.e. above the threshold value). When considering the outputs of the geostatistical model (Fig. 1a), 30 % of the surface of France has PAH concentrations in soils higher than the background value of  $100 \mu\text{g kg}^{-1}$ . To better assess the risk of exceeding this background value, we used a geostatistical model to map the probability that the  $\Sigma 15$  PAHs concentration in soils exceeds  $100 \mu\text{g kg}^{-1}$  (Fig. 1b). Industrialised regions in northern France exhibit probabilities of exceeding  $100 \mu\text{g kg}^{-1}$  above 0.8. High probabilities of soils exceeding the threshold value were also found in the vicinity of the biggest cities in France, such as Paris, Marseille, Lyon, Nantes, La Rochelle, and Bordeaux (Fig. 1b).

### 3.2.2 Enhancing spatial predictions

To take into account the uncertainty of the local mean, the ordinary multi-Gaussian kriging (Emery, 2006) was tested, but there is no significant difference from the standard conditional expectation presented here, as the ordinary kriging is very close to the simple kriging due to regular sampling. The

variogram model of the latent Gaussian variable presents a significant nugget effect, which may result from local contamination or measurement errors, as previously mentioned. This introduces the issue of the support considered for the measurement ( $20 \text{ m} \times 20 \text{ m}$ ) and for the interpolated grid (with a mesh of  $2000 \text{ m} \times 2000 \text{ m}$ ), taking into account that the support and measurement errors in the Gaussian model may improve the spatial definition (see Chilès and Delfiner, 2012, for a review of models for support changes and example applications).

The standard empirical variogram averages the squared differences from different zones; the variogram model is isotropic and stationary, but final maps suggest a north–south (or northwestern–southeastern) contrast and local anisotropies, which may or may not be partially explained by external covariates (e.g. topography, distance to the sea, and dominant wind direction). Hence, modelling local anisotropies (Fouedjio et al., 2016) or using a nonstationary stochastic partial differential equation (SPDE) model (Pereira, 2019) could improve the structured part of the variogram model and, hence, the maps.

### 3.3 Major origin of PAHs using molecular diagnostic ratios

To identify the origin of PAHs in French soils, the four widely used molecular diagnostic ratios –  $\text{Flh} / (\text{Flh} + \text{Py})$ ,  $\text{Ant} / (\text{Ant} + \text{Phe})$ ,  $\text{BaA} / (\text{BaA} + \text{Chry})$ , and  $\text{IdP} / (\text{IdP} + \text{BghiP})$  – were investigated to distinguish among petrogenic (i.e. crude oil), pyrogenic (coal, wood, and biomass combustion), and fossil fuel combustion sources (Table 6). We computed these ratios and mapped the results using a simple point map (Fig. 2) without any interpolation, and missing values corresponded to sites at which none of the PAHs used in the ratios were quantified.

The spatial distribution of the four diagnostic ratios appears to be similar to the majority of calculated ratios in the northern part of France (Fig. 2) but with different indicators with respect to the PAH origins. The values of the  $\text{Flh} / (\text{Flh} + \text{Py})$ ,  $\text{IdP} / (\text{IdP} + \text{BghiP})$ , and  $\text{BaA} / (\text{BaA} + \text{Chry})$  ratios are mainly associated with pyrogenic signatures attributed to coal, wood, and biomass burning (Fig. 2a, c, d), whereas the  $\text{Ant} / (\text{Ant} + \text{Phe})$  values indicate petrogenic signatures attributed to crude oil (Fig. 2b). This difference in the PAH origins, based on the  $\text{Ant} / (\text{Ant} + \text{Phe})$  ratio, could be explained by the sensitivity of this ratio to environmental processes such as oxidation or biodegradation (Katsoyiannis and Breivik, 2014; Tobiszewski and Namieśnik, 2012). Phenanthrene and anthracene are lighter PAHs susceptible to multiple processes during their transport, shifting the source signature of  $\text{Ant} / (\text{Ant} + \text{Phe})$  (Biache et al., 2014; Zhang et al., 2005). The lower detection of anthracene (8 %) compared to phenanthrene (55 %), resulting in many instances of  $\text{Ant} / (\text{Ant} + \text{Phe})$  being close to 0, probably reflects an-

**Table 6.** Most commonly used molecular diagnostic ratios associated with PAH origins.

Ratio	Petrogenic	Fossil fuel combustion	Pyrogenic	References
Flh / (Flh + Py)	0–0.4	0.4–0.5	0.5–1	Biache et al. (2014),
Ant / (Ant + Phe)	0–0.1		0.1–1	Ravindra et al. (2008),
BaA / (BaA + Chry)	0–0.2	0.2–0.35	0.35–1	Tobiszewski and Namieśnik (2012),
IdP (IdP + BghiP)	0–0.2	0.2–0.5	0.5–1	Yunker et al. (2002); Zhang et al. (2005)

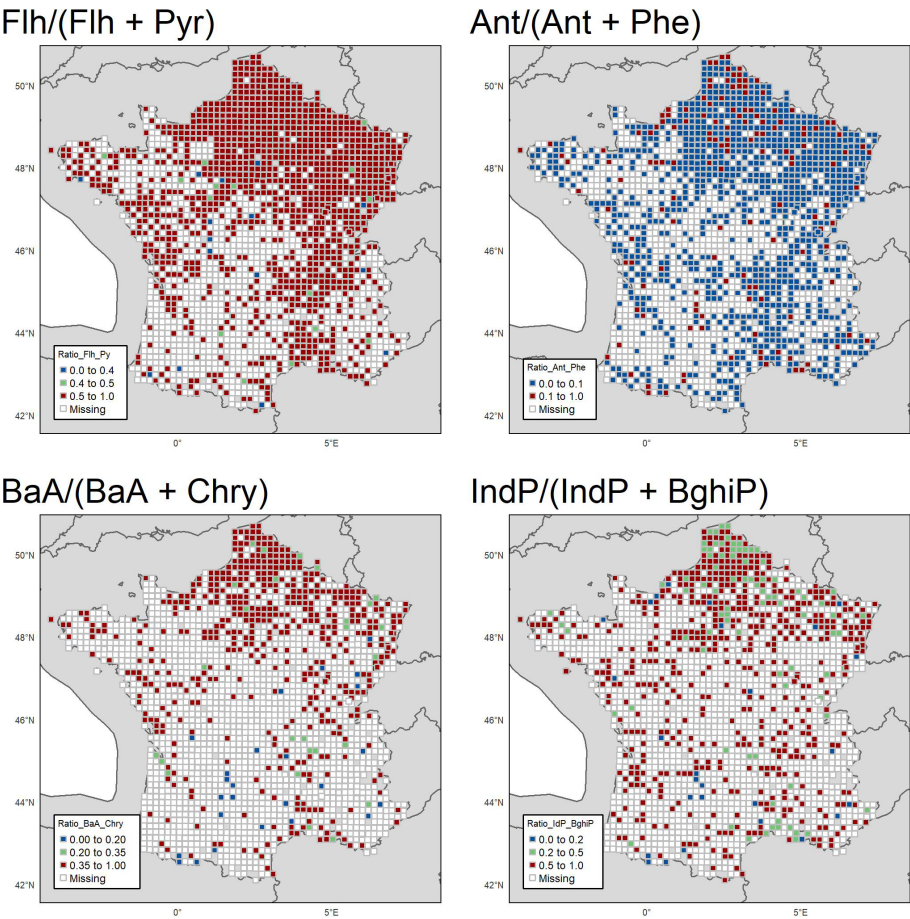


**Figure 2.** Spatialised molecular diagnostic ratios in French soils. Missing values correspond to sites at which none of the PAHs used in the ratios were quantified.

thracene depletion rather than PAH origins. Consequently, Ant / (Ant + Phe) should be used with caution when trying to identify the origin of PAHs and was thus considered an unreliable source signature in this study.

As shown by the Flh / (Flh + Py), IdP / (IdP + BghiP), and BaA / (BaA + Chry) diagnostic ratios (Fig. 2a, c, and d), pyrogenic combustion, such as coal and wood burning, might be the main origin of PAHs measured in the soil of the north-eastern part of France and the Rhône Valley in the southeast. In the literature, Flh / (Flh + Py) and IdP / (IdP + BghiP) have been identified as the most conservative ratios due to the lower sensitivity of Flh, Py, IdP, and BghiP to degradation (Brändli et al., 2008; Tobiszewski and Namieśnik,

2012). In the case of BaA / (BaA + Chry), shifts in the signature have been observed during atmospheric transport due to photodegradation (Katsoyiannis and Breivik, 2014); however, the concordance of the latter ratio with the PAH origins identified using the Flh / (Flh + Py) and IdP / (IdP + BghiP) diagnostic ratios suggests that it is a reliable molecular diagnostic ratio in this study. The spatial trend exhibited by the Flh / (Flh + Py) ratio for the sites with nonmissing values, combined with IdP / (IdP + BghiP) and BaA / (BaA + Chry) ratios, seems to confirm the pyrogenic origin of PAHs in the north of France, despite the substantial number of missing values for IdP / (IdP + BghiP) and BaA / (BaA + Chry) due to a lower detection of the PAH molecule used in these ratios.

In addition to the indication of pyrogenic origins of the PAHs by molecular diagnostic ratios, the homogeneous spatial pattern of both PAH concentrations and the ratio in north-eastern France (Figs. 1 and 2) suggest contamination linked to regional atmospheric emissions, with the latter being the major source of soil PAHs (Tobiszewski and Namieśnik, 2012). Multiple studies reported high PAH deposition rates in western Europe from 1900 to 1970 due to industrial development, especially from heavy industries (e.g. coal and steel), with a massive peak in 1960 before a decrease due to pollution control (Elmqvist et al., 2007; Fernández et al., 2000; Gabrieli et al., 2010; Leorri et al., 2014). An estimation of the BaP emissions in Europe by Pacyna et al. (2003) identified Germany, France, and the UK as the main contributors, emitting 22 %, 8 %, and 11 % of the 1300 t of BaP released in 1970, respectively. In addition, the Gabrieli et al. (2010) study of atmospheric PAH deposition beginning in 1700 showed that, during 1900–1960, the  $\text{Flh} / (\text{Flh} + \text{Py})$  ratio decreased from 0.65 to 0.55. This decreasing trend was explained by the increasing contribution of fossil fuel combustion (gasoline and diesel) to local atmospheric PAH deposition (Gabrieli et al., 2010). This value of 0.6 in  $\text{Flh} / (\text{Flh} + \text{Py})$  appears to be the main value in the northeastern part of France (Fig. 2a), therefore supporting historical industrial PAH emissions as a major source of PAHs in the soils of this region. This hypothesis of the coal industry's contribution to PAH loads in northern France during the mid-20th century was also suggested by Lorgeoux et al. (2016), using organic pollutant records from a sediment core of the Seine estuary.

The persistence of PAHs over more than a century and the absence of changes in the signature could be explained by multiple factors. First, the amount of PAHs emitted at the beginning of the 20th century was 10 to 100 times higher than the current PAH depositions (Fernández et al., 2000; Gabrieli et al., 2010). The high rates of PAH deposition during those 30 to 60 years could have prevented any changes in the PAH signatures in soils associated with source modifications after 1960 due to the stock of PAHs already polluting soils (Froger et al., 2019; Gateuille et al., 2014b). Second, the process of PAH sequestration in the soil could explain their long-term persistence in French soils (Biache et al., 2011). This sequestration is caused by the sorption of PAHs on organic matter and their diffusion through micropores in soils, reducing their bioavailability for microorganisms (Bogan and Sullivan, 2003; Semple et al., 2003). Overall, the ageing of soils could increase PAH interactions in soils, enhancing the slow but irreversible sequestration of PAHs and reducing their potential degradation in soils (Anyanwu and Semple, 2015; Duan et al., 2015; Ma et al., 2012; Ouvrard et al., 2013).

Additionally, the hot spots of PAH concentrations around major cities (Fig. 1) suggests local sources of contaminants, such as in urban or suburban environments, and multiple sources of PAHs could contribute to PAH soil contamination.

Current sources of PAHs, such as road traffic, local industries, and residential emissions (household heating; Cachada et al., 2012a; Gateuille et al., 2014a; Lohmann et al., 2000), as well as legacy contamination due to former industries (Bertrand et al., 2015; Pies et al., 2007), could contribute to soil PAH content. However, precise source identification and apportionment cannot be done based only on PAH molecular diagnostic ratios, which only provide information about pyrogenic, petrogenic, or mixed PAHs in soils (Brändli et al., 2008; Tobiszewski and Namieśnik, 2012; Yunker et al., 2014). Multivariate analysis associated with linear mixing models and positive matrix factorisation could be performed to reveal PAH sources and their respective contributions to PAH contamination in soils (Harrison et al., 1996; Larsen and Baker, 2003; Wang et al., 2015). Additionally, each PAH molecule may present different spatial structures, depending on its source. Minimum and maximum auto-correlation factors (Petitgas et al., 2018; Switzer and Green, 1984) deduced from different indicators (for example, the indicators of the  $1_{\text{PAHi}} \geq \text{LOC}_{\text{LOQ}}$ ) could be used. These factors are the spatial counterpart of the standard principal component analysis (PCA), and their mapping could help regionalise the origin of PAHs and estimate the risk using alternate nonlinear methods such as discrete disjunctive kriging. Finally, other fingerprinting methods involving new analyses, such as carbon isotopes (Kim et al., 2008; Petrišić et al., 2013; Zhang et al., 2020) or alkyl PAHs (Morales-Caselles et al., 2017; Yuan et al., 2015), could be used to complete source identification and apportionment.

### 3.4 Health risk assessment

#### 3.4.1 Total lifetime cancer risks in France

The results of the health risk assessment evaluated for the residential population are presented in Table 7. According to the US Environmental Protection Agency, the elevated risk is attributed to a TLCR above 10 000, meaning that the probability of an individual developing cancer over a lifetime is more than one in 10 000. A TLCR value under 1 000 000 is considered to indicate virtual safety, meaning that the probability of an individual developing cancer is less than one in 1 000 000. Consequently, TLCRs between  $10^{-4}$  and  $10^{-6}$  were associated with a moderate risk. However, the limit of  $10^{-6}$  is commonly used by the USEPA as the target risk value to calculate screening levels in soils. In France, the ministerial circular on 10 December 1999 chose a value of  $10^{-5}$  as the limit defining the sites needing remediation for polluted soils.

Among the 2154 soils collected throughout the French territory, 54 % had a TLCR value (i.e. 1512 sites), indicating that those soils were contaminated by at least one of the seven carcinogenic PAHs. TLCR values for the residential population ranged from  $1.89 \times 10^{-11}$  to  $1.37 \times 10^{-5}$ , with 20 sites presenting TLCRs above the safety target value of  $10^{-6}$ .

**Table 7.** Summary of the total lifetime cancer risk (TLCR) attributed to French soils for the residential population.

	TLCR residential population
Min	$1.89 \times 10^{-11}$
Max	$1.37 \times 10^{-5}$
Mean	$1.13 \times 10^{-7}$
Q25	$3.82 \times 10^{-9}$
Q50	$1.07 \times 10^{-8}$
Q75	$9.63 \times 10^{-8}$
No. of sites $< 10^{-7}$	1144
No. of sites between $10^{-7}$ and $10^{-6}$	348
No. of sites $> 10^{-6}$	20

(i.e. 1 % of the sites). Only one site showed a TLCR value above  $10^{-5}$ , which was considered a polluted site according to French legislation. Ingestion of soil contributed to 68.8 % of the total cancer risk compared to dermal contact (31.2 %) and inhalation (0.01 %), which is commonly observed in the literature (Tong et al., 2018; Wang et al., 2017b).

Considering that soil samples were collected mainly in locations distant from anthropogenic sources (both industries and urban areas), the current study could be considered an evaluation of the background level of PAHs in French soils. Consequently, soils contaminated by PAHs showed low risks for residential populations, considering that 99 % of the soils presented TLCR values under  $10^{-6}$  (Table 7). In the literature, higher TLCR values have been identified in southern Italy, with mean ILCRs of  $4.77 \times 10^{-6}$  for adults (Qi et al., 2020), and in China, with a mean TLCR value of  $1.86 \times 10^{-6}$  in Shanghai (Tong et al., 2018) and an ILCR value of  $4.4 \times 10^{-5}$  in the Yangtze River Delta (Wang et al., 2017b). However, those studies were conducted mainly in industrial and highly urbanised regions and reflect the risks induced by soils under high anthropogenic pressure and not the background contamination over a large territory.

Figure 3 presents the residential maps of TLCRs and indicates that the northeastern part of France and the Rhône Valley had the most sites with estimated TLCRs reflecting the national PAH concentration distribution (Fig. 1a). These observations can be explained by the positive correlation between the BaP toxic equivalent and the  $\Sigma 15$  PAHs shown in Fig. 4. These results indicate that the contamination of soils by PAHs is driven by the most carcinogenic PAHs with the highest toxic equivalent factors (TEFs; i.e. BaA, Chr, BbF, BkF, BaP, IndP, and DahA), whose concentrations are proportional to the total PAHs measured.

The soils with TLCRs between  $10^{-7}$  and  $10^{-6}$  are concentrated in the northern part of France and in the vicinity of the main cities (Fig. 3). Among the 17 main cities shown in Fig. 3, 11 are located in areas in which TLCRs could be calculated, and four are situated in areas with mul-

tiples sites with TLCRs between  $10^{-7}$  and  $10^{-6}$ . As multiple sources of PAHs are concentrated in urban areas, soils with higher contamination levels that are usually found in cities might pose higher risks to the population, such as in Naples, where the ILCRs were above  $1 \times 10^{-5}$  (Albanese et al., 2015). In France, a database of 300 urban soils was created (ADEME, 2018), and the soils therein had a median value of  $1560 \mu\text{g kg}^{-1}$  in the  $\Sigma 16$  PAHs, which is 50 times higher than the  $32 \mu\text{g kg}^{-1}$  in the  $\Sigma 15$  PAHs in the current study. Therefore, the higher risks posed by PAHs in soils would be expected in urbanised regions. In addition, the distribution of soils with higher TLCRs around cities (especially Paris, Lille, and Marseille) highlights the influence of densely urbanised areas on the surrounding soils over a distance of up to several dozen kilometres (Jensen et al., 2007). Finally, the 20 sites with the highest TLCRs above  $10^{-6}$  appeared to be randomly distributed throughout the territory, suggesting local sources of PAHs at those sites, such as heavy industries.

The first results of the background national health risks linked to PAHs show the spatial heterogeneity in the risks encountered by the population and the necessity of considering soils in risk evaluations and the national surveillance of contaminants in the environment.

### 3.4.2 Limits and perspectives

As we used a site-specific determinist method to predict the TLCR at each site, the variations in the population characteristics and model parameters were not integrated in the calculation. Therefore, the use of a probabilistic model with a sensitivity analysis would result in more accurate predictions of cancer risks based on French population statistics (USEPA, 2001; Bruce et al., 2007; Tong et al., 2018). However, the use of the point estimate approach is the first step recommended by the USEPA (2001) when conducting risk assessments. These results provided an overview of the health risks associated with background PAH concentrations in French soils and the need to further evaluate these risks.

A total of three pathways of human exposure to PAHs in the soils were considered (i.e. ingestion, dermal contact, and inhalation). To integrate all exposure routes, PAH transfer from soil to food production (crops, vegetables, and fruits) should be taken into account, in addition to groundwater transfer. Many studies have demonstrated that exposure through food ingestion significantly contributes to the total risk, as in the Yangtze River Delta, where TLCRs rose from  $4.4 \times 10^{-5}$  to  $9.17 \times 10^{-4}$  (Wang et al., 2017b). Similarly, in southern Italy, the risk induced by food ingestion exceeded the risks of the other pathways by 2 orders of magnitude (Qi et al., 2020). Therefore, the potential risks posed by PAHs in French soils could be underestimated, especially since a significant part of the production of cereals (soft wheat and barley) and some vegetables (potato) are cultivated in northern France. Consequently, a more in-depth health risk study inte-



## Risk for residents

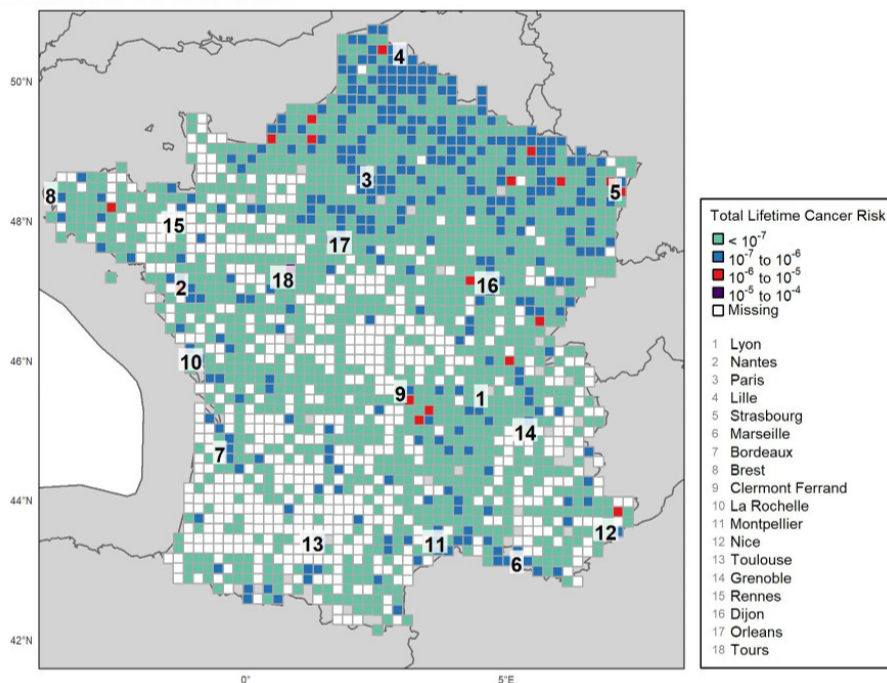


**Figure 3.** Health risk assessment for the residential population, showing the total lifetime cancer risk (TLCR) for French soils, along with the location of major cities. Missing values correspond to sites at which no PAHs were quantified, so a TLCR below  $10^{-7}$  can be assumed.

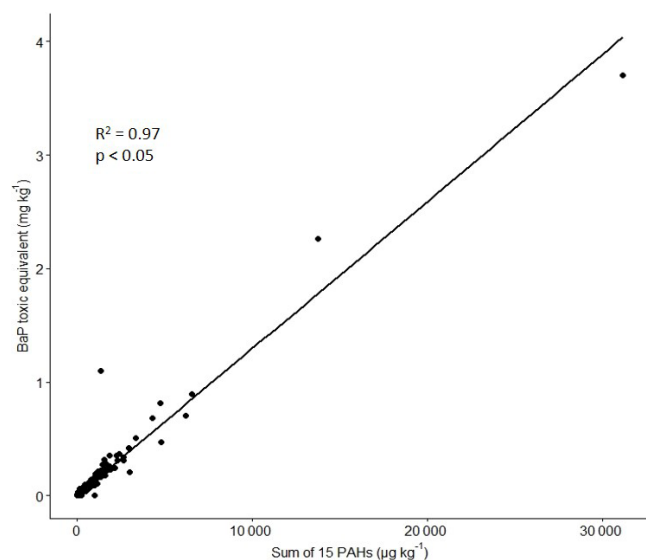


**Figure 4.** Correlation between the BaPeq in milligrams per kilogram and the concentration of the  $\Sigma 15$  PAHs in micrograms per kilogram in French soils.

grating land use types (crops, grassland, and forest), produce cultivation, and a scenario in which the residential population raises their own vegetables would result in deeper insight into the risks induced by PAHs in soils.

The risk estimations were made based on the additional toxic effects of PAHs using TEFs. However, little is known about the potential synergistic, antagonist, or additive effects of PAH mixtures on the human body, which could lead to either underestimation or overestimation of ILCRs. In addition, the proportion of PAHs absorbed in the body resulting in harmful effects is considered to be 100 %; however, Hack and Selenka (1996) identified the influence of food type on the mobilisation of PAHs from soil in the digestive tract. Therefore, the population's diet could also influence the potential risks associated with soil contaminants. Consequently, to better evaluate the risk induced by food ingestion, bioavailability tests should be conducted using the standard diet of the targeted population. Furthermore, as PAHs in French soils were identified as originating from historical contamination, the ageing process might reduce PAH bioavailability (Bogan and Sullivan, 2003; Semple et al., 2003) and their potential toxicity to organisms (Duan et al., 2015; Ma et al., 2012). Nevertheless, Reeves et al. (2001) demonstrated the low impact of soil ageing on PAH availability and ingestion by organisms (i.e. rats in the study).

Finally, the sequestration of PAHs in the soil could result in the biodegradation of some molecules into metabolites such as fluoranthene-2,3-dione (F23Q), which is known to be toxic, can accumulate in the environment, and inhibits the degradation of other PAHs (Kazunga et al., 2001). This issue was also reported by Schmidt et al. (2010), who demon-

strated that fungal PAH metabolites tend to accumulate in the soil solution due to their high water solubility and appear to mineralise more slowly than the parent PAHs potentially leaching into the groundwater. These results support the need to study the fate of contaminants in soils and their associated risks.

## 4 Conclusions

This study explored the concentrations of PAHs in 2154 soils collected throughout France based on an extended data set collected using a systematic sampling grid covering all land use types. A total of 70 % of the soil samples presented PAH concentrations over the LOQ, and 30 % of those soils were above the background value of  $100 \mu\text{g kg}^{-1}$  in the  $\Sigma 15$  PAHs, with a probability of 0.8 to exceed this threshold value in northern France. The spatial distribution of the  $\Sigma 15$  PAHs throughout the country showed a particular pattern, with higher PAH content in soils situated in the north-eastern part of France, in the Rhône Valley, and near the main cities. These results demonstrated large-scale contamination of French soils by PAHs, which was identified by PAH molecular ratios as being legacy contamination from the emissions linked to the industrialisation of Europe that started in 1850. The health risk assessment conducted for the residential population showed that 99 % of the French soils presented a risk lower than the target value of TLCR of  $10^{-6}$  for the residential population. Only one site exceeded the limit of  $10^{-5}$  chosen by the French government to consider soil as contaminated in residential areas. A higher density of TLCRs between  $10^{-7}$  and  $10^{-6}$  was found in the northeastern part of France, the Rhône Valley, and in soils surrounding the main cities. These results demonstrate the need to investigate the risk associated with PAHs in soils, using a probabilistic method, with French population statistics that includes food ingestion as a transfer pattern. Finally, this study demonstrated the heterogeneous risks associated with PAHs in soils over France, highlighted the environmental inequalities with regional variations in population and ecosystem exposure to hazardous contaminants, and indicated the need to conduct large-scale studies to understand contaminant behaviours, their fates in the ecosystem, and their associated risks.

**Code availability.** The R code used to spatialise the data has been published in a repository of the research institute INRAE. This code can be accessed through the following DOI: <https://doi.org/10.15454/BJFUEV> (Saby et al., 2021).

**Data availability.** The data used in the paper are available at: <https://doi.org/10.15454/WPR2C9> (Froger et al., 2021). A raster file in Geotiff format containing the geo-referenced data of PAH sums after spatialisation is also available with the data set.

**Supplement.** The supplement related to this article is available online at: <https://doi.org/10.5194/soil-7-161-2021-supplement>.

**Author contributions.** CF and NPAS conceptualised the paper and curated the data, and CF wrote the original draft. NPAS developed the methodology with GC, XF, HR, and FM, and NPAS conducted the formal analysis with CdF and XF. NPAS, LB, AB, and CCJ supervised. NPAS, CCJ, LB, GC, XF, CdF, HR, FM, and HB reviewed and edited the paper. GC found the resources and conducted the validation with XF, CdF, HR, and FM. XF and CdF developed the software.

**Competing interests.** The authors declare that they have no conflict of interest.

**Acknowledgements.** The soil sampling and the analyses of physicochemical properties of soils were supported by the French Scientific Group of Interest on soils, GIS Sol, involving the French Ministry in charge of the Ecological Transition (MTE), the French Ministry in charge of the Agriculture and Food (MAA), the French Agency for Environment and Energy Management (ADEME), the French Biodiversity Agency (OFB), the National Institute of Geographic and Forest Information (IGN), the French National Research Institute for Sustainable Development, and the National Institute for Agronomic and Environmental Research (INRAE). We thank all the soil surveyors and technical assistants involved in sampling the sites.

**Financial support.** The PAH analyses were supported by a grant from the French Observatory for the Pesticide Residues (ORP).

**Review statement.** This paper was edited by Raúl Zornoza and reviewed by Ivan Alekseev and Yong Zhang.

## References

- ADEME: Méthodologie de détermination des valeurs de fonds dans les sols: Echelle territoriale, Groupe de travail sur les valeurs de fonds, 112 pp., 2018.
- Aichner, B., Bussian, B., Lehnik-Habrink, P., and Hein, S.: Levels and spatial distribution of persistent organic pollutants in the environment: A case study of German forest soils, *Environ. Sci. Technol.*, 47, 12703–12714, <https://doi.org/10.1021/es4019833>, 2013.
- Albanese, S., Fontaine, B., Chen, W., Lima, A., Cannatelli, C., Piccolo, A., Qi, S., Wang, M., and De Vivo, B.: Polycyclic aromatic hydrocarbons in the soils of a densely populated region and associated human health risks: the Campania Plain (Southern Italy) case study, *Environ. Geochem. Hlth.*, 37, 1–20, <https://doi.org/10.1007/s10653-014-9626-3>, 2015.
- Anyanwu, I. N. and Semple, K. T.: Fate and behaviour of nitrogen-containing polycyclic aromatic hydrocar-

- bons in soil, *Environ. Technol. Innov.*, 3, 108–120, <https://doi.org/10.1016/j.eti.2015.02.006>, 2015.
- Bertrand, O., Mondamert, L., Grosbois, C., Dhivert, E., Bourrain, X., Labanowski, J., and Desmet, M.: Storage and source of polycyclic aromatic hydrocarbons in sediments downstream of a major coal district in France, *Environ. Pollut.*, 207, 329–340, <https://doi.org/10.1016/j.envpol.2015.09.028>, 2015.
- Biache, C., Ghislain, T., Faure, P., and Mansuy-Huault, L.: Low temperature oxidation of a coking plant soil organic matter and its major constituents: An experimental approach to simulate a long term evolution, *J. Hazard. Mater.*, 188, 221–230, <https://doi.org/10.1016/j.jhazmat.2011.01.102>, 2011.
- Biache, C., Mansuy-Huault, L., and Faure, P.: Impact of oxidation and biodegradation on the most commonly used polycyclic aromatic hydrocarbon (PAH) diagnostic ratios: Implications for the source identifications, *J. Hazard. Mater.*, 267, 31–39, <https://doi.org/10.1016/j.jhazmat.2013.12.036>, 2014.
- Bogan, B. W. and Sullivan, W. R.: Physicochemical soil parameters affecting sequestration and mycobacterial biodegradation of polycyclic aromatic hydrocarbons in soil, *Chemosphere*, 52, 1717–1726, [https://doi.org/10.1016/S0045-6535\(03\)00455-7](https://doi.org/10.1016/S0045-6535(03)00455-7), 2003.
- Brändli, R. C., Bucheli, T. D., Ammann, S., Desaulles, A., Keller, A., Blum, F., and Stahel, W. A.: Critical evaluation of PAH source apportionment tools using data from the Swiss soil monitoring network, *J. Environ. Monitor.*, 10, 1278–1286, <https://doi.org/10.1039/b807319h>, 2008.
- Bruce, E. D., Abusalih, A. A., McDonald, T. J., and Autenrieth, R. L.: Comparing deterministic and probabilistic risk assessments for sites contaminated by polycyclic aromatic hydrocarbons (PAHs), *J. Environ. Sci. Heal. A*, 42, 697–706, <https://doi.org/10.1080/10934520701304328>, 2007.
- Brus, D. J., Lamé, F. P. J., and Nieuwenhuis, R. H.: National baseline survey of soil quality in the Netherlands, *Environ. Pollut.*, 157, 2043–2052, <https://doi.org/10.1016/j.envpol.2009.02.028>, 2009.
- Bull, S. and Collins, C.: Promoting the use of BaP as a marker for PAH exposure in UK soils, *Environ. Geochem. Hlth.*, 35, 101–109, <https://doi.org/10.1007/s10653-012-9462-2>, 2013.
- Cachada, A., Pato, P., Rocha-Santos, T., da Silva, E. F., and Duarte, A. C.: Levels, sources and potential human health risks of organic pollutants in urban soils, *Sci. Total Environ.*, 430, 184–192, <https://doi.org/10.1016/j.scitotenv.2012.04.075>, 2012a.
- Cachada, A., Pereira, M. E., da Silva, E. F., and Duarte, A. C.: Sources of potentially toxic elements and organic pollutants in an urban area subjected to an industrial impact, *Environ. Monit. Assess.*, 184, 15–32, <https://doi.org/10.1007/s10661-011-1943-8>, 2012b.
- Cachada, A., da Silva, E. F., Duarte, A. C., and Pereira, R.: Risk assessment of urban soils contamination: The particular case of polycyclic aromatic hydrocarbons, *Sci. Total Environ.*, 551–552, 271–284, <https://doi.org/10.1016/j.scitotenv.2016.02.012>, 2016.
- Canadian Council of Ministers of the Environment (CCME): Canadian Soil Quality Guidelines for Carcinogenic and Other Polycyclic Aromatic Hydrocarbons (Environmental and Human Health Effects), Scientific Criteria Document (revised), 216 pp., 2010.
- Carre, F., Caudeville, J., Bonnard, R., Bert, V., Boucard, P., and Ramel, M.: Soil Contamination and Human Health: A Major Challenge for Global Soil Security, in: *Global Soil Security*, edited by: Field, D. J., Morgan, C. L. S., and McBratney, A. B., Springer Int. Publishing AG, Cham, Switzerland, 275–295, 2017.
- Chilès, J.-P. and Delfiner, P.: *Geostatistics: Modeling Spatial Uncertainty*, edn. 2, John Wiley & Sons Inc., Hoboken, New Jersey, USA, 2012.
- Cui, S., Zhang, Z., Fu, Q., Hough, R., Yates, K., Osprey, M., Yakowa, G., and Coull, M.: Long-term spatial and temporal patterns of polycyclic aromatic hydrocarbons (PAHs) in Scottish soils over 20 years (1990–2009): A national picture, *Geoderma*, 361, 114135, <https://doi.org/10.1016/j.geoderma.2019.114135>, 2020.
- Desaulles, A., Ammann, S., Blum, F., Brändli, R., and Bucheli, T. D.: Teneurs en HAP et en PCB dans les sols en Suisse, Résultats de l’Observatoire national des sols 1995/1999, *Obs. Natl. des sols*, 96 pp., available at: <http://www.nabo.admin.ch> (last access: 20 May 2021), 2010.
- Duan, L., Naidu, R., Thavamani, P., Meaklim, J., and Megharaj, M.: Managing long-term polycyclic aromatic hydrocarbon contaminated soils: a risk-based approach, *Environ. Sci. Pollut. R.*, 22, 8927–8941, <https://doi.org/10.1007/s11356-013-2270-0>, 2015.
- Elmqvist, M., Zencak, Z., and Gustafsson, Ö.: A 700 year sediment record of black carbon and polycyclic aromatic hydrocarbons near the EMEP air monitoring station in Aspvreten, Sweden, *Environ. Sci. Technol.*, 41, 6926–6932, <https://doi.org/10.1021/es070546m>, 2007.
- Emery, X.: Ordinary multigaussian kriging for mapping conditional probabilities of soil properties, *Geoderma*, 132, 75–88, <https://doi.org/10.1016/j.geoderma.2005.04.019>, 2006.
- Fernández, P., Vilanova, R. M., Martínez, C., Appleby, P., and Grimalt, J. O.: The Historical Record of Atmospheric Pyrolytic Pollution over Europe Registered in the Sedimentary PAH from Remote Mountain Lakes, *Environ. Sci. Technol.*, 34, 1906–1913, <https://doi.org/10.1021/es9912271>, 2000.
- Flipo, N., Labadie, P., and Lestel, L. (Eds.): Correction to: The Seine River Basin, in: *The Seine River Basin, The Handbook of Environmental Chemistry*, vol. 90. Springer, Cham., [https://doi.org/10.1007/698\\_2020\\_667](https://doi.org/10.1007/698_2020_667), 2020.
- Fouedjio, F., Desassis, N., and Rivoirard, J.: A generalized convolution model and estimation for non-stationary random functions, *Spat. Stat.-Neth.*, 16, 35–52, <https://doi.org/10.1016/j.spasta.2016.01.002>, 2016.
- Froger, C., Quantin, C., Gasperi, J., Caupos, E., Monvoisin, G., Evrard, O., and Ayrault, S.: Impact of urban pressure on the spatial and temporal dynamics of PAH fluxes in an urban tributary of the Seine River (France), *Chemosphere*, 219, 1002–1013, <https://doi.org/10.1016/j.chemosphere.2018.12.088>, 2019.
- Froger, C., Saby, N., Jolivet, C., Boulonne, L., Freulon, X., de Fouquet, C., Roussel, H., Marot, F., and Bispo, A.: Données de réplification pour: Spatial variations, origins, and risk assessments of polycyclic aromatic hydrocarbons in French soils, *Portail Data INRAe [data set]*, <https://doi.org/10.15454/WPR2C9>, 2021.
- Gabrieli, J., Vallenga, P., Cozzi, G., Gabrielli, P., Gambaro, A., Sigl, M., Decet, F., Schwikowski, M., Gäggeler, H., Boutron, C., Cescon, P., and Barbante, C.: Post 17th-century changes of european pah emissions recorded in high-altitude alpine snow and ice, *Environ. Sci. Technol.*, 44, 3260–3266, <https://doi.org/10.1021/es903365s>, 2010.

- Gaspéri, J., Ayrault, S., Moreau-Guigon, E., Alliot, F., Labadie, P., Budzinski, H., Blanchard, M., Muresan, B., Caupos, E., Cladière, M., Gateuille, D., Tassin, B., Bordier, L., Teil, M.-J., Bourges, C., Desportes, A., Chevreuil, M., and Moilleron, R.: Contamination of soils by metals and organic micropollutants: case study of the Parisian conurbation, *Environ. Sci. Pollut. R.*, 25, 23559–23573, <https://doi.org/10.1007/s11356-016-8005-2>, 2018.
- Gateuille, D., Evrard, O., Lefevre, I., Moreau-Guigon, E., Alliot, F., Chevreuil, M., and Mouchel, J.-M.: Combining measurements and modelling to quantify the contribution of atmospheric fallout, local industry and road traffic to PAH stocks in contrasting catchments, *Environ. Pollut.*, 189, 152–160, <https://doi.org/10.1016/j.envpol.2014.02.029>, 2014a.
- Gateuille, D., Evrard, O., Lefevre, I., Moreau-Guigon, E., Alliot, F., Chevreuil, M., and Mouchel, J.-M.: Mass balance and decontamination times of Polycyclic Aromatic Hydrocarbons in rural nested catchments of an early industrialized region (Seine River basin, France), *Sci. Total Environ.*, 470–471, 608–617, <https://doi.org/10.1016/j.scitotenv.2013.10.009>, 2014b.
- Gocht, T., Ligouis, B., Hinderer, M., and Grathwohl, P.: Accumulation of Polycyclic aromatic Hydrocarbons in rural Soils based on Mass balances at the Catchment scale, *Environ. Toxicol. Chem.*, 26, 591–600, <https://doi.org/10.1897/06-287R.1>, 2007.
- Grimmer, G.: PAH – Their contribution to the carcinogenicity of various emissions, *Toxicol. Environ. Chem.*, 10, 171–181, <https://doi.org/10.1080/02772248509357101>, 1985.
- Gubler, A., Wächter, D., Blum, F., and Bucheli, T. D.: Remarkably constant PAH concentrations in Swiss soils over the last 30 years, *Environ. Sci.-Proc. Imp.*, 17, 1816–1828, <https://doi.org/10.1039/c5em00344j>, 2015.
- Hack, A. and Selenka, F.: Mobilization of PAH and PCB from contaminated soil using a digestive tract model, *Toxicol. Lett.*, 88, 199–210, [https://doi.org/10.1016/0378-4274\(96\)03738-1](https://doi.org/10.1016/0378-4274(96)03738-1), 1996.
- Harrison, R. M., Smith, D. J. T., and Luhana, L.: Source apportionment of atmospheric polycyclic aromatic hydrocarbons collected from an urban location in Birmingham, U.K., *Environ. Sci. Technol.*, 30, 825–832, 1996.
- Heywood, E., Wright, J., Wienburg, C. L., Black, H. I. J., Long, S. M., Osborn, D., and Spurgeon, D. J.: Factors influencing the national distribution of polycyclic aromatic hydrocarbons and polychlorinated biphenyls in British soils, *Environ. Sci. Technol.*, 40, 7629–7635, <https://doi.org/10.1021/es061296x>, 2006.
- IRIS, NCEA and U.S. EPA: Executive summary, *New Dir. Youth Dev.*, 2008, 7–12, <https://doi.org/10.1002/yd.282>, 2008.
- Jensen, H., Reimann, C., Finne, T. E., Ottesen, R. T., and Arnoldussen, A.: PAH-concentrations and compositions in the top 2 cm of forest soils along a 120 km long transect through agricultural areas, forests and the city of Oslo, Norway, *Environ. Pollut.*, 145, 829–838, <https://doi.org/10.1016/j.envpol.2006.05.008>, 2007.
- Katsoyiannis, A. and Breivik, K.: Model-based evaluation of the use of polycyclic aromatic hydrocarbons molecular diagnostic ratios as a source identification tool, *Environ. Pollut.*, 184, 488–494, <https://doi.org/10.1016/j.envpol.2013.09.028>, 2014.
- Kavouras, I. G., Koutrakis, P., Tsapakis, M., Lagoudaki, E., Stephanou, E. G., Von Baer, D., and Oyola, P.: Source Apportionment of Urban Particulate Aliphatic and Polynuclear Aromatic Hydrocarbons (PAHs) Using Multivariate Methods, *Environ. Sci. Technol.*, 35, 2288–2294, <https://doi.org/10.1021/es001540z>, 2001.
- Kazunga, C., Aitken, M. D., Gold, A., and Sangaiah, R.: Fluoranthene-2,3- and -1,5-diones are novel products from the bacterial transformation of fluoranthene, *Environ. Sci. Technol.*, 35, 917–922, <https://doi.org/10.1021/es001605y>, 2001.
- Keyte, I. J., Albinet, A., Harrison, R. M., and Harrison, R. M.: On-road traffic emissions of polycyclic aromatic hydrocarbons and their oxy- and nitro-derivative compounds measured in road tunnel environments, *Sci. Total Environ.*, 566–567, 1131–1142, <https://doi.org/10.1016/j.scitotenv.2016.05.152>, 2016.
- Killops, S. D. and Massoud, M. S.: Polycyclic aromatic hydrocarbons of pyrolytic origin in ancient sediments: evidence for Jurassic vegetation fires, *Org. Geochem.*, 18, 1–7, [https://doi.org/10.1016/0146-6380\(92\)90137-M](https://doi.org/10.1016/0146-6380(92)90137-M), 1992.
- Kim, M., Kennicutt, M. C., and Qian, Y.: Source characterization using compound composition and stable carbon isotope ratio of PAHs in sediments from lakes, harbor, and shipping waterway, *Sci. Total Environ.*, 389, 367–377, <https://doi.org/10.1016/j.scitotenv.2007.08.045>, 2008.
- Lark, R.: Modelling complex soil properties as contaminated regionalized variables, *Geoderma*, 106, 173–190, [https://doi.org/10.1016/S0016-7061\(01\)00123-9](https://doi.org/10.1016/S0016-7061(01)00123-9), 2002.
- Larsen, R. K. and Baker, J. E.: Source Apportionment of Polycyclic Aromatic Hydrocarbons in the Urban Atmosphere: A Comparison of Three Methods, *Environ. Sci. Technol.*, 37, 1873–1881, <https://doi.org/10.1021/es0206184>, 2003.
- Leorri, E., Mitra, S., Irabien, M. J., Zimmerman, A. R., Blake, W. H., and Cearreta, A.: A 700 year record of combustion-derived pollution in northern Spain: Tools to identify the Holocene/Anthropocene transition in coastal environments, *Sci. Total Environ.*, 470–471, 240–247, <https://doi.org/10.1016/j.scitotenv.2013.09.064>, 2014.
- Liu, G., Niu, J., Guo, W., An, X., and Zhao, L.: Ecological and health risk-based characterization of agricultural soils contaminated with polycyclic aromatic hydrocarbons in the vicinity of a chemical plant in China, *Chemosphere*, 163, 461–470, <https://doi.org/10.1016/j.chemosphere.2016.08.056>, 2016.
- Lohmann, R., Northcott, G. L., and Jones, K. C.: Assessing the contribution of diffuse domestic burning as a source of PCDD/Fs, PCBs, and PAHs to the U.K. Atmosphere, *Environ. Sci. Technol.*, 34, 2892–2899, <https://doi.org/10.1021/es991183w>, 2000.
- Lorgeoux, C., Moilleron, R., Gasperi, J., Ayrault, S., Bonté, P., Lefevre, I., Tassin, B., Bonté, P., Lefevre, I., and Tassin, B.: Temporal trends of persistent organic pollutants in dated sediment cores: Chemical fingerprinting of the anthropogenic impacts in the Seine River basin, Paris, *Sci. Total Environ.*, 541, 1355–1363, <https://doi.org/10.1016/j.scitotenv.2015.09.147>, 2016.
- Ma, L., Zhang, J., Han, L., Li, W., Xu, L., Hu, F., and Li, H.: The effects of aging time on the fraction distribution and bioavailability of PAH, *Chemosphere*, 86, 1072–1078, <https://doi.org/10.1016/j.chemosphere.2011.11.065>, 2012.
- Ma, W. L., Liu, L. Y., Tian, C. G., Qi, H., Jia, H. L., Song, W. W., and Li, Y. F.: Polycyclic aromatic hydrocarbons in Chinese surface soil: occurrence and distribution, *Environ. Sci. Pollut. R.*, 22, 4190–4200, <https://doi.org/10.1007/s11356-014-3648-3>, 2015.
- Maliszewska-Kordybach, B.: Polycyclic aromatic hydrocarbons in agricultural soils in Poland: preliminary proposals for criteria to



- evaluate the level of soil contamination, *Appl. Geochem.*, 11, 121–127, [https://doi.org/10.1016/0883-2927\(95\)00076-3](https://doi.org/10.1016/0883-2927(95)00076-3), 1996.
- Maliszewska-Kordybach, B.: Persistent Organic Contaminants in the Environment: PAHs as a Case Study, in: *Bioavailability of Organic Xenobiotics in the Environment*, edited by: Baveye, P., Block, J. C., and Goncharuk, V. V., NATO ASI Series (Series 2: Environment), Springer, Dordrecht, the Netherlands, 3–34, [https://doi.org/10.1007/978-94-015-9235-2\\_1](https://doi.org/10.1007/978-94-015-9235-2_1), 1999.
- Maliszewska-Kordybach, B., Smreczak, B., Klimkowicz-Pawlas, A., and Terelak, H.: Monitoring of the total content of polycyclic aromatic hydrocarbons (PAHs) in arable soils in Poland, *Chemosphere*, 73, 1284–1291, <https://doi.org/10.1016/j.chemosphere.2008.07.009>, 2008.
- MINES ParisTech/ARMINES: RGeostats: The Geostatistical R Package, Version: 12.0.1, available at: <http://cg.ensmp.fr/rgeostats> (last access: 31 May 2021), 2020.
- Morales-Caselles, C., Yunker, M. B., and Ross, P. S.: Identification of Spilled Oil from the MV Marathassa (Vancouver, Canada 2015) Using Alkyl PAH Isomer Ratios, *Arch. Environ. Con. Tox.*, 73, 118–130, <https://doi.org/10.1007/s00244-017-0390-0>, 2017.
- Morillo, E., Romero, A. S., Madrid, L., Villaverde, J., and Maqueda, C.: Characterization and sources of PAHs and potentially toxic metals in urban environments of Sevilla (southern Spain), *Water Air Soil Poll.*, 187, 41–51, <https://doi.org/10.1007/s11270-007-9495-9>, 2008.
- Motelay-Massei, A., Ollivon, D., Garban, B., Teil, M. J., Blanchard, M., and Chevreuil, M.: Distribution and spatial trends of PAHs and PCBs in soils in the Seine River basin, France, *Chemosphere*, 55, 555–565, <https://doi.org/10.1016/j.chemosphere.2003.11.054>, 2004.
- Ouvrard, S., Chenot, E.-D., Masfaraud, J.-F., and Schwartz, C.: Long-term assessment of natural attenuation: statistical approach on soils with aged PAH contamination, *Biodegradation*, 24, 539–548, <https://doi.org/10.1007/s10532-013-9618-5>, 2013.
- Pacyna, J. M., Breivik, K., Münch, J., and Fudala, J.: European atmospheric emissions of selected persistent organic pollutants, 1970–1995, *Atmos. Environ.*, 37, 119–131, [https://doi.org/10.1016/S1352-2310\(03\)00240-1](https://doi.org/10.1016/S1352-2310(03)00240-1), 2003.
- Pereira, M.: Generalized random fields on Riemannian manifolds: theory and practice, PSL Research University, Paris, France, available at: <https://pastel.archives-ouvertes.fr/tel-02499376> (last access: 23 June 2020), 2019.
- Petitgas, P., Woillez, M., Doray, M., and Rivoirard, J.: Handbook of geostatistics in R for fisheries and marine ecology, Indicator-Based Geostatistical Models For Mapping Fish Survey Data, *Math. Geosci.*, 50, 187–208, <https://doi.org/10.1007/s11004-018-9725-2>, 2018.
- Petitgas, P., Woillez, M., Doray, M., and Rivoirard, J.: Indicator-Based Geostatistical Models For Mapping Fish Survey Data, *Math. Geosci.*, 50, 187–208, <https://doi.org/10.1007/s11004-018-9725-2>, 2018.
- Petrišič, M. G., Muri, G., and Ogrinc, N.: Source identification and sedimentary record of polycyclic aromatic hydrocarbons in lake bled (NW Slovenia) using stable carbon isotopes, *Environ. Sci. Technol.*, 47, 1280–1286, <https://doi.org/10.1021/es303832v>, 2013.
- Pies, C., Yang, Y., and Hofmann, T.: Distribution of polycyclic aromatic hydrocarbons (PAHs) in floodplain soils of the Mosel and Saar River, *J. Soils Sediments*, 7, 216–222, <https://doi.org/10.1065/jss2007.06.233>, 2007.
- Qi, P., Qu, C., Albanese, S., Lima, A., Cicchella, D., Hope, D., Cerino, P., Pizzolante, A., Zheng, H., Li, J., and De Vivo, B.: Investigation of polycyclic aromatic hydrocarbons in soils from Caserta provincial territory, southern Italy: Spatial distribution, source apportionment, and risk assessment, *J. Hazard. Mater.*, 383, 121158, <https://doi.org/10.1016/j.jhazmat.2019.121158>, 2020.
- Ravindra, K., Sokhi, R., and Vangrieken, R.: Atmospheric polycyclic aromatic hydrocarbons: Source attribution, emission factors and regulation, *Atmos. Environ.*, 42, 2895–2921, <https://doi.org/10.1016/j.atmosenv.2007.12.010>, 2008.
- Reeves, W. R., McDonald, T. J., Bordelon, N. R., George, S. E., and Donnelly, K. C.: Impacts of aging on in vivo and in vitro measurements of soil-bound polycyclic aromatic hydrocarbon availability, *Environ. Sci. Technol.*, 35, 1637–1643, <https://doi.org/10.1021/es0017110>, 2001.
- Rivoirard, J.: Introduction to disjunctive kriging and non-linear geostatistics, California University, Clarendon Press, 180 pp., 1994.
- Rivoirard, J. and Romary, T.: Continuity for Kriging with Moving Neighborhood, *Math. Geosci.*, 43, 469–481, <https://doi.org/10.1007/s11004-011-9330-0>, 2011.
- Saby, N., Freulon, X., and Froger, C.: R code for the statistical analysis for: Spatial variations, origins, and risk assessments of polycyclic aromatic hydrocarbons in French soils, Portail Data INRAE [code], V2, <https://doi.org/10.15454/BJFUEV>, 2021.
- Schmidt, S. N., Christensen, J. H., and Johnsen, A. R.: Fungal PAH-metabolites resist mineralization by soil microorganisms, *Environ. Sci. Technol.*, 44, 1677–1682, <https://doi.org/10.1021/es903415t>, 2010.
- Semple, K. T., Morriss, A. W. J., and Paton, G. I.: Bioavailability of hydrophobic organic contaminants in soils: fundamental concepts and techniques for analysis, *Eur. J. Soil Sci.*, 54, 809–818, 2003.
- Switzer, P. and Green, A.: Min/max autocorrelation factors for multivariate spatial imagery, Technical report No. 6, Computer Science and Statistics, Vol. 16, 16 pp., 1984.
- Tobiszewski, M. and Namieśnik, J.: PAH diagnostic ratios for the identification of pollution emission sources, *Environ. Pollut.*, 162, 110–119, <https://doi.org/10.1016/j.envpol.2011.10.025>, 2012.
- Tong, R., Yang, X., Su, H., Pan, Y., Zhang, Q., Wang, J., and Long, M.: Levels, sources and probabilistic health risks of polycyclic aromatic hydrocarbons in the agricultural soils from sites neighboring suburban industries in Shanghai, *Sci. Total Environ.*, 616–617, 1365–1373, <https://doi.org/10.1016/j.scitotenv.2017.10.179>, 2018.
- USEPA: Human Health Evaluation Manual Part (B, Development of Risk-based Preliminary Remediation Goals), Risk Assess. Guid. Superfund, I(December), 66, available at: <https://nepis.epa.gov/Exe/ZyPDF.cgi/100020LF.PDF?Dockey=100020LF.PDF> (last access: 12 September 2020), 1991.
- USEPA: Soil Screening Guidance: User's Guide, Environmental Protection Agency, 1–49, Washington DC, USA, available at: [https://rais.ornl.gov/documents/SSG\\_nonrad\\_user.pdf](https://rais.ornl.gov/documents/SSG_nonrad_user.pdf) (last access: 12 September 2020), 1996.
- USEPA: Risk Assessment Guidance for Superfund (RAGS) Volume III – Part A: Process for Conducting Probabilistic Risk As-

- assessment, Appendix B, Risk Assess. Guid. Superfund, 1–385, available at: [http://www.epa.gov/sites/production/files/2015-09/documents/rags3adt\\_complete.pdf](http://www.epa.gov/sites/production/files/2015-09/documents/rags3adt_complete.pdf) (last access: 15 September 2020), 2001.
- USEPA: Regional Screening Levels (RSLs), U.S. Environmental Protection Agency, Washington DC, available at: <https://www.epa.gov/risk/regional-screening-levels-rsls-users-guide>, last access: 1 October 2020.
- Villanneau, E., Saby, N. P. A., Arrouays, D., Jolivet, C. C., Boulonne, L., Caria, G., Barriuso, E., Bispo, A., and Briand, O.: Spatial distribution of lindane in top-soil of Northern France, *Chemosphere*, 77, 1249–1255, <https://doi.org/10.1016/j.chemosphere.2009.08.060>, 2009.
- Villanneau, E. J., Saby, N. P. A., Orton, T. G., Jolivet, C. C., Boulonne, L., Caria, G., Barriuso, E., Bispo, A., Briand, O., and Arrouays, D.: First evidence of large-scale PAH trends in French soils, *Environ. Chem. Lett.*, 11, 99–104, <https://doi.org/10.1007/s10311-013-0401-y>, 2013.
- Wang, C., Wu, S., Zhou, S., Wang, H., Li, B., Chen, H., Yu, Y., and Shi, Y.: Polycyclic aromatic hydrocarbons in soils from urban to rural areas in Nanjing: Concentration, source, spatial distribution, and potential human health risk, *Sci. Total Environ.*, 527–528, 375–383, <https://doi.org/10.1016/j.scitotenv.2015.05.025>, 2015.
- Wang, C., Wu, S., Zhou, S., Shi, Y., and Song, J.: Characteristics and Source Identification of Polycyclic Aromatic Hydrocarbons (PAHs) in Urban Soils: A Review, *Pedosphere*, 27, 17–26, [https://doi.org/10.1016/S1002-0160\(17\)60293-5](https://doi.org/10.1016/S1002-0160(17)60293-5), 2017a.
- Wang, J., Zhang, X., Ling, W., Liu, R., Liu, J., Kang, F., and Gao, Y.: Contamination and health risk assessment of PAHs in soils and crops in industrial areas of the Yangtze River Delta region, China, *Chemosphere*, 168, 976–987, <https://doi.org/10.1016/j.chemosphere.2016.10.113>, 2017b.
- Wang, X.-T., Miao, Y., Zhang, Y., Li, Y.-C., Wu, M.-H., and Yu, G.: Polycyclic aromatic hydrocarbons (PAHs) in urban soils of the megacity Shanghai: Occurrence, source apportionment and potential human health risk, *Sci. Total Environ.*, 447, 80–89, <https://doi.org/10.1016/j.scitotenv.2012.12.086>, 2013.
- Webster, R. and Oliver, M.: *Geostatistics for Environmental Scientists*, 2nd Edn., Wiley, Chichester, England, 315 pp., 2007.
- Wenzel, K. D., Manz, M., Hubert, A., and Schüürmann, G.: Fate of POPs (DDX, HCHs, PCBs) in upper soil layers of pine forests, *Sci. Total Environ.*, 286, 143–154, [https://doi.org/10.1016/S0048-9697\(01\)00972-X](https://doi.org/10.1016/S0048-9697(01)00972-X), 2002.
- Yang, W., Lang, Y., and Li, G.: Cancer risk of polycyclic aromatic hydrocarbons (PAHs) in the soils from Jiaozhou Bay wetland, *Chemosphere*, 112, 289–295, <https://doi.org/10.1016/j.chemosphere.2014.04.074>, 2014.
- Yang, Y., Ligouis, B., Pies, C., Achten, C., and Hofmann, T.: Identification of carbonaceous geosorbents for PAHs by organic petrography in river floodplain soils, *Chemosphere*, 71, 2158–2167, <https://doi.org/10.1016/j.chemosphere.2008.01.010>, 2008.
- Yu, L., Duan, L., Naidu, R., and Semple, K. T.: Abiotic factors controlling bioavailability and bioaccessibility of polycyclic aromatic hydrocarbons in soil: Putting together a bigger picture, *Sci. Total Environ.*, 613–614, 1140–1153, <https://doi.org/10.1016/j.scitotenv.2017.09.025>, 2018.
- Yuan, K., Wang, X., Lin, L., Zou, S., Li, Y., Yang, Q., and Luan, T.: Characterizing the parent and alkyl polycyclic aromatic hydrocarbons in the Pearl River Estuary, Daya Bay and northern South China Sea: Influence of riverine input, *Environ. Pollut.*, 199, 66–72, <https://doi.org/10.1016/j.envpol.2015.01.017>, 2015.
- Yunker, M. B., Macdonald, R. W., Vingarzan, R., Mitchell, R. H., Goyette, D., and Sylvestre, S.: PAHs in the Fraser River basin: a critical appraisal of PAH ratios as indicators of PAH source and composition, *Org. Geochem.*, 33, 489–515, [https://doi.org/10.1016/S0146-6380\(02\)00002-5](https://doi.org/10.1016/S0146-6380(02)00002-5), 2002.
- Yunker, M. B., McLaughlin, F. A., Fowler, M. G., and Fowler, B. R.: Source apportionment of the hydrocarbon background in sediment cores from Hecate Strait, a pristine sea on the west coast of British Columbia, Canada, *Org. Geochem.*, 76, 235–258, <https://doi.org/10.1016/j.orggeochem.2014.08.010>, 2014.
- Zhang, R., Li, T., Russell, J., Zhang, F., Xiao, X., Cheng, Y., Liu, Z., Guan, M., and Han, Q.: Source apportionment of polycyclic aromatic hydrocarbons in continental shelf of the East China Sea with dual compound-specific isotopes ( $\delta^{13}\text{C}$  and  $\delta^2\text{H}$ ), *Sci. Total Environ.*, 704, 135459, <https://doi.org/10.1016/j.scitotenv.2019.135459>, 2020.
- Zhang, X. L., Tao, S., Liu, W. X., Yang, Y., Zuo, Q., and Liu, S. Z.: Source Diagnostics of Polycyclic Aromatic Hydrocarbons Based on Species Ratios: A Multimedia Approach, *Environ. Sci. Technol.*, 39, 9109–9114, <https://doi.org/10.1021/es0513741>, 2005.
- Zheng, T., Ran, Y., and Chen, L.: Polycyclic aromatic hydrocarbons (PAHs) in rural soils of Dongjiang River Basin: Occurrence, source apportionment, and potential human health risk, *J. Soils Sediments*, 14, 110–120, <https://doi.org/10.1007/s11368-013-0753-8>, 2014.